10th International Conference on Composite Science and Technology
ICCST/10
A.L. Araújo, J.R. Correia, C.M. Mota Soares, et al. (Editors)

TECHNIQUES TO INVESTIGATE VISCOELASTICALLY GENERATED PRESTRESS IN POLYMERIC COMPOSITES

Chao Ge[*], Bing Wang[†], Kevin S. Fancey[†]

[*]School of Mechatronical Engineering
Beijing Institute of Technology
Beijing, China
gechao@bit.edu.cn

[*†]School of Engineering
University of Hull
Hull, HU6 7RX, U.K.
c.ge@hull.ac.uk
b.wang@2013.hull.ac.uk
k.s.fancey@hull.ac.uk

Key words: Polymer composites, Prestress, Microhardness, Charge storage.

Summary: *A viscoelastically prestressed polymeric matrix composite (VPPMC) is produced by subjecting polymeric fibres to tensile creep, the applied load being removed before the fibres are moulded into a resin matrix. Following matrix curing, the viscoelastically strained fibres impart compressive stresses to the surrounding matrix, counterbalanced by residual tension in the fibres. Using VPPMCs based on nylon 6,6 fibres in polyester resin, improved mechanical properties have been observed, compared with control (unstressed) counterparts; e.g. increases of up to 50% in impact toughness and flexural stiffness. Although there is some understanding of the force output/time properties from viscoelastically recovering fibres, little is known of the fibre-matrix interactions and resulting prestress characteristics within VPPMCs. In this paper, two methods for addressing these aspects are investigated: (i) the SEMME (scanning electron microscope mirror effect) and (ii) Vickers microhardness indentation. By comparing results from VPPMC samples of varying fibre volume fraction with their control counterparts, initial findings from (i) suggest that there are fewer trapped negative charges in VPPMC samples, implying that these possess higher fibre-matrix interfacial strengths than the control samples. For (ii), a significant increase in measured microhardness is observed in VPPMC samples, and this can be attributed to the effects of compressive stresses within the matrix, produced by the viscoelastically recovering fibres. The findings from these two methods are considered in the context of previous research into VPPMC mechanical performance characteristics.*

1 INTRODUCTION

A viscoelastically prestressed polymeric matrix composite (VPPMC) is produced by subjecting polymeric fibres to tensile creep; the applied load is then removed before the fibres are moulded into a resin matrix. Following matrix curing, the viscoelastically strained fibres impart compressive stresses to the surrounding matrix, counterbalanced by residual

tension in the fibres. Using VPPMCs based on nylon 6,6 fibres in polyester or epoxy resin, improved mechanical properties have been observed, compared with control (unstressed) counterparts. Thus increases of up to 50% in impact toughness and flexural stiffness [1-6] and strength, modulus and energy absorption exceeding 15%, 30% and 40% respectively from tensile tests [7] have been observed.

A similar state of prestress can also be achieved with elastically prestressed PMCs (EPPMCs); here, the prestress is produced by maintaining an elastic tensile strain on fibres during matrix curing. For unidirectional continuous fibre EPPMCs, mechanical property improvements [8-10] are comparable to those of VPPMCs. There are however two potential drawbacks with EPPMCs. First, fibre length, orientation and spatial distribution are restricted by the need to apply fibre tension whilst the matrix cures; these restrictions can compromise fibre and mould geometries for more complex situations. Clearly, VPPMC processing has no such restrictions, since fibre stretching and moulding operations are decoupled. Second, since the matrix is polymeric, localised creep at the fibre-matrix interface regions can be expected, in response to compressive stresses imposed by the fibres. Therefore, the prestress effect within an EPPMC may deteriorate with time [2]. In contrast, accelerated ageing studies have demonstrated no deterioration in VPPMC mechanical performance (Charpy impact toughness) over a duration equivalent to 25 years at a constant 50 ℃ ambient [11].

Although the main body of VPPMC research has been based on prestress provided by nylon 6,6 fibres [1-7, 11], other researchers have successfully demonstrated VPPMCs based on bamboo, showing an increase in flexural toughness of 28% [12]. Most recently, increases of 20-40% in flexural modulus and impact toughness from VPPMCs based on ultra-high molecular weight polyethylene (UHMWPE) fibres have been achieved [13, 14]. There have also been investigations into the force output-time characteristics from viscoelastically recovering fibres of nylon 6,6 [15] and UHMWPE [13, 14]: e.g. for nylon 6,6, the viscoelastic recovery force increased with time (t) and was predicted to reach a limiting value of 12 MPa across the fibre ends as t approached infinity [15].

Despite the progress in research into the mechanical performance characteristics of VPPMCs, little is known of the fibre-matrix interactions and resulting prestress characteristics within these composite materials. In this paper, two methods for addressing these aspects are investigated: (i) the scanning electron microscope mirror effect (SEMME) and (ii) Vickers microhardness indentation.

2 BACKGROUND

2.1 The scanning electron microscope mirror effect

The SEMME technique can provide information related to the trapping and mobility of electric charges within insulating materials. This has been used to investigate the dielectric behaviour of fibre-reinforced composites, such as glass fibre/epoxy resin [16] and hemp fibre/polypropylene [17]. In these studies, the fibre/matrix interface regions have been observed to play a major role in the trapping or diffusion of charges, where charge diffusion is associated with high interface strength. Therefore, since viscoelastically generated stresses are created at the fibre/matrix interface regions in our composites, the SEMME technique may provide further insight into the role of these stresses on mechanical performance.

The principle of the SEMME method involves irradiating an insulating sample in an SEM with a high voltage (10s of kV) over a controlled injection time, t_i. During injection, negative charges are locally trapped and stabilised within the sample and these produce an electric

field in the vacuum (sample) chamber of the SEM. If the sample is subsequently observed with a lower energy electron beam (100s of volts), electrons from this beam can be reflected from an equipotential surface produced by the electric field, as illustrated in Figure 1(a). Thus effectively, the arrangement is analogous to the behaviour of a convex mirror in visible light. The resulting mirror image can be observed on the SEM viewing screen as a distorted view of the SEM vacuum chamber, as shown in Figure 1(b).

The central black disc, shown in Figure 1(b), represents the exit orifice of the electron beam in the mirror image, and has an apparent diameter, d. The size of d increases with decreasing electron beam energy, V, used for producing the mirror image, since the position of the equipotential surface causing beam reflection will depend on the beam energy used. Thus $1/d = f(V)$ and the following relationship has been established by Vallayer [18]:

$$\frac{1}{d} = \frac{4L}{d_r} \cdot \frac{2\pi\varepsilon_0(\varepsilon_r + 1)}{K \cdot Q_t} \cdot V \qquad (1)$$

Here, d_r = the real diameter of the exit orifice, L = the SEM working distance, Q_t = quantity of negative electric charge trapped and stabilised in the sample (which produces the electric field), and K = a parameter dependent on SEM chamber characteristics; ε_0 and ε_r are the permittivities of free space and sample material (relative) respectively.

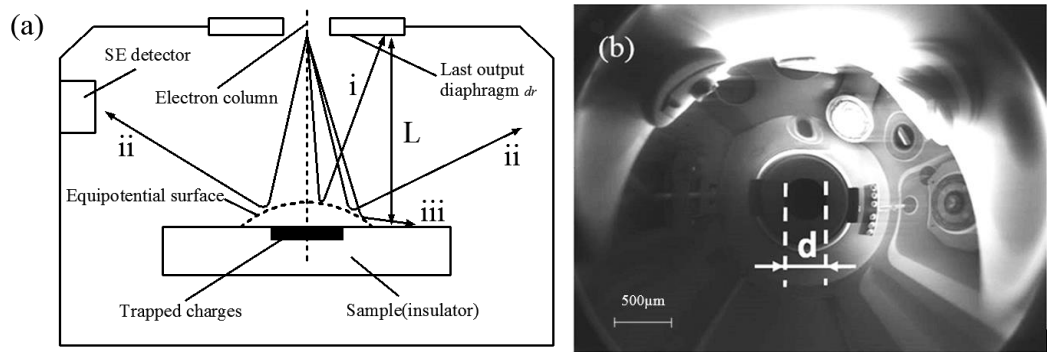

Figure 1: The SEMME method. (a) Schematic of how trapped charges (following high voltage injection) within an insulating sample create an electric field, producing an electrostatic convex mirror. Electrons bounce off an equipotential surface, following either path (i) to give the central black disc in (b), or (ii) to give a mirror image of the chamber walls in (b), or (iii) to give a distorted image of the sample (re-drawn from [16]). (b) Typical SEMME image taken from our chamber.

For mirror images produced at low beam voltages, a linear relationship can be expected from a plot of $1/d$ versus V, and the quantity of trapped charge, Q_t, can be determined from the gradient. Thus a steeper gradient represents a lower value of Q_t, implying that fewer charges are trapped and stabilised; instead, charges become more diffused through the material. For fibre-reinforced PMCs, there is evidence to suggest that diffusion of charges along the fibre-matrix interfaces, as opposed to trapping in these regions, corresponds to higher interfacial shear strength [16, 17]. At higher beam voltages, the plot of $1/d$ versus V becomes non-linear, a sub-linear curve indicating a lateral spreading of charges as opposed to a deeper diffusion of charges implied by a super-linear curve [16].

Clearly, for VPPMC samples, the $1/d$ versus V characteristics, when compared with equivalent data from control samples, may provide information on the effects of prestress at the fibre-matrix interface regions. This in turn could improve our understanding of viscoelastically generated prestress mechanisms on composite mechanical properties.

2.2 Vickers microhardness indentation

The use of Vickers microhardness indentation is a widely used method for characterising solid materials, as it is simple and inexpensive. Since it only involves deformation of a very small material volume, it can also be considered as being non-destructive. Its primary use however, is for the characterisation of metals and ceramics; hence published information on its application to polymeric materials is relatively sparse. This can be attributed to the changes in indentation geometry on a polymeric surface, which can occur through (i) elastic recovery, occurring immediately after the indentation process and (ii) viscoelastically induced recovery, which causes more gradual changes with time. Although indentation geometry is affected, the change in dimensions of the diagonals is very small and can be neglected, which makes it possible to measure the hardness of polymers [19, 20].

The Vickers microhardness test consists of indenting the material with a diamond indenter utilising a certain load for a certain duration and calculating hardness by measuring the geometrical parameters of these indentations. The diamond indenter has the shape of a pyramid with a square base and an angle of 136 ° between opposite faces, as shown in Figure 2(a). After indentation on materials by a load *P*, the hardness HV is then calculated by dividing *P* by the surface area of the indentation:

$$\mathrm{HV} = 2\sin(\frac{136}{2})\frac{P}{d_1 \cdot d_2} \tag{2}$$

where d_1 and d_2 are lengths of the diagonals.

As a result of viscoelastically generated prestress, microhardness data from VPPMC samples might be different to that obtained from control (no prestress) samples. Moreover, the viscoelastic nature of polymeric composites, coupled with prestress effects, may show different changes in indentation geometry over time between VPPMC and control samples.

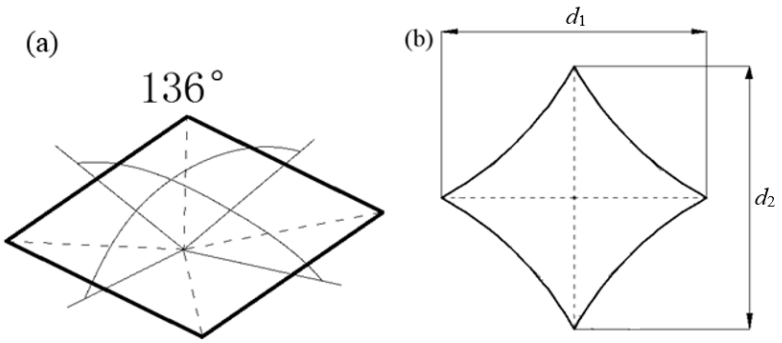

Figure 2: Illustration of: (a) geometry of the Vickers indenter; (b) measured indentation parameters.

By comparing results from VPPMC samples of varying fibre volume fraction with their control counterparts, an increase in measured microhardness is expected to be observed in VPPMC samples, and this can be attributed to the effects of compressive stress within the matrix, produced by the viscoelastically recovering fibres.

3 EXPERIMENTAL

3.1 Production of samples

VPPMC sample preparation followed that described in previously published papers [1-7] and is briefly presented here. First, continuous multifilament nylon 6,6 yarn (140 filaments, 26 μm fibre diameter, 94 tex), supplied by Ogden Fibres Ltd, UK, was annealed in a fan assisted oven (150 ℃, 0.5 h) for production of both test (prestressed) and control (non-prestressed) samples. Following this, yarn for test samples was attached to a stretching rig and subjected to a 330 MPa tensile creep stress for 24 h while yarn for control samples was positioned in close proximity to the stretching rig for exposure to the same ambient environment (20-21 ℃, 30-40% RH). Immediately after the load was removed, both yarns were cut into multiple lengths and brushed into flat ribbons ready for moulding.

The matrix was a clear-casting resin, Reichhold Polylite 32032, mixed with 2% MEKP catalyst, supplied by MB Fibreglass, UK. Gel time for this resin was ~30 min and had sufficiently cured after 2 hours (at room temperature), to permit demoulding. Two identical aluminium moulds, each with a 10 mm wide and 3 mm deep channel, were used so that a strip of test and control material could be cast simultaneously from the same resin mix. Following demoulding, the test and control strips were each cut into five samples with dimensions of 80 × 10 × 3.2 mm, as shown in Figure 3. The batch of 5 test and 5 control samples was then held under weighted steel strip for 24 h to prevent potential bending effects from internal stresses. The samples were stored in polythene bags (to minimise contamination) at room temperature (18-22 ℃) for 336 hours (2 weeks) prior to being used for tests. One batch of samples, with a fibre volume fraction (V_f) of 2% was produced for the SEMME study and two batches, with V_f values of 2% and 15%, were produced for the microhardness measurements.

For microhardness investigations, a further five resin-only samples (i.e. no fibres) were produced, using the same moulding procedures outlined above. Also, a sample of 1.6 mm diameter nylon 6,6 monofilament, obtained from Goodfellow Cambridge Ltd, UK, was annealed under the same conditions as the nylon fibre. This was then cut into short lengths (~20 mm) and moulded as a bundle, using the polyester resin, to produce a cylindrically-shaped moulding that was then ground and polished.

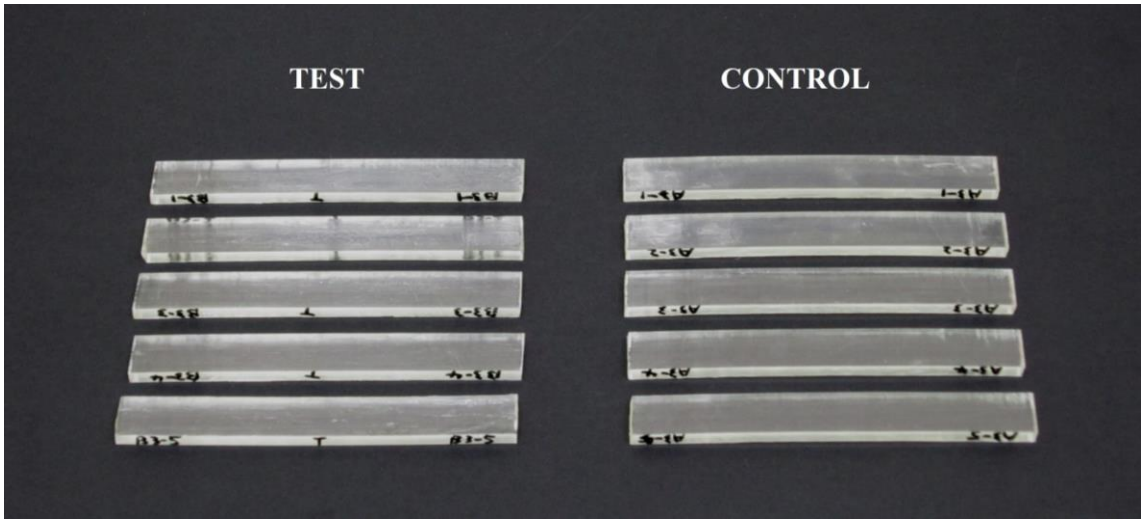

Figure 3: A typical batch of test (prestressed) and control (non-prestressed) samples.

3.2 SEMME tests

To conduct the mirror effect tests, an S360 SEM (Electron Microscopy Ltd., Cambridge,

UK) was employed. As a result of using open cast moulding, fibres tended to settle towards the bottom of the mould prior to curing, thereby increasing fibre spatial density towards one side of the samples. Thus all samples were tested with the fibre-rich surface facing uppermost to the electron beam.

The samples were first irradiated in the SEM at 20 kV in focused mode for 10 seconds (t_i) using a beam blanking device. The samples were then observed with a lower energy voltage ranging from 200-1000 V with the working distance, L, fixed at 23 mm. The apparent diameter, d, was measured at each voltage value. The five test and five control samples were tested only once, to avoid any influences from previous charging effects. From this, a mean value of d could be determined at each voltage setting, for both test and control samples.

3.3 Vickers microhardness testing

The indentation process was conducted on a Leitz Miniload 2 microhardness tester and, as for the SEMME analysis, samples were tested on the fibre-rich side. For repeatability, two microhardness readings per sample were made at random locations. Thus with 5 test and 5 control samples, a mean value for the prestressed and non-prestressed cases were each obtained from a total of 10 measurements. A similar number of microhardness measurements were made on the resin-only samples and also on the nylon 6,6 monofilament cross-sections at the ground/polished surface of the cylindrical moulding. All measurements were performed with a 55 g indentation load.

As stated in Section 2.2, time-dependent changes in indentation geometry can occur with polymeric materials, even though diagonal dimensions remain relatively stable. Specifically, the recovery process over time usually results in a pyramidal indentation having sides that become inwardly concaved to produce a star-shaped indentation [19, 20]. Therefore, this effect may be used to characterise the recovery process and prestress state in VPPMCs. Thus, in addition to microhardness measurements, the changes in indentation shape over time were monitored. Initial observations were taken 7 minutes after load removal, then observations were made every 30 minutes for 4 hours. A CCD camera mounted on a Nikon microscope (400x magnification) in DIC (Differential Interference Contrast) mode, in combination with the ImagePro software, was used for this purpose.

4 RESULTS AND DISCUSSION

4.1 SEMME analysis

Figure 4 shows the mirror curves from the test and control samples. Both linear and curved regions are observed, which provides information on diffusion, stability and localisation of trapped charges within VPPMCs and their control counterparts.

The gradient of the test samples in the linear region is steeper than that of the control samples. Since the test and control samples were moulded simultaneously, have the same V_f and were tested under identical conditions, their permittivities are assumed to be similar. Thus according to Eq. (1), the steeper gradient for the test samples suggests that there are fewer trapped and stabilised charges, Q_t, located in the injection point regions. Although there are a limited number of data points within the linear regions of Figure 4, approximate linear fits give gradients of 0.0066 (test) and 0.0049 (control). Thus based on Eq. (1), there is a decrease of ~26% in the amount of trapped charges within the test samples, compared with corresponding control samples.

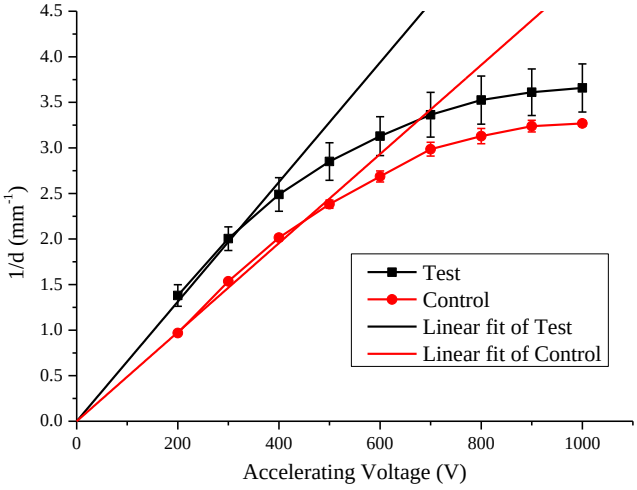

Figure 4: Plots of 1/*d* versus accelerating voltage *V* for 2.0% V_f test (prestressed) and control (non-prestressed) samples; error bars represent standard error of the mean values (5 readings per data point). Both linear and sub-linear regions are observed.

As stated in Section 2.1, charge diffusion, which can be expected to occur along the fibre-matrix interfaces, as opposed to charge trapping, is associated with higher interfacial shear strength. Therefore, these results suggest that viscoelastically generated prestress may improve shear strength at the fibre-matrix interfaces. Charge diffusion along the fibre-matrix interfaces in favour of charge trapping must be attributed to compressive stresses imparted by the viscoelastically strained fibres as they attempt strain recovery against the surrounding matrix material. It may be speculated that the prestress effect reduces the availability of interfacial defects capable of trapping charges and that this reduction in defects improves fibre-matrix interfacial adhesion. On a macroscopic level, an improvement in interfacial shear strength due to viscoelastically generated prestress can be readily associated with the observed increases in, for example, tensile strength and flexural stiffness from VPPMCs that have been previously reported [6, 7].

In addition to the linear regions, Figure 4 shows that the curved regions are sub-linear for both test and control samples. As noted in Section 2.1, this implies a lateral spreading of charges, which may be explained by the electrons being injected perpendicular to fibres; the trapped charges will diffuse along the fibre/matrix interfaces, resulting in lateral diffusion [16].

4.2 Vickers microhardness tests

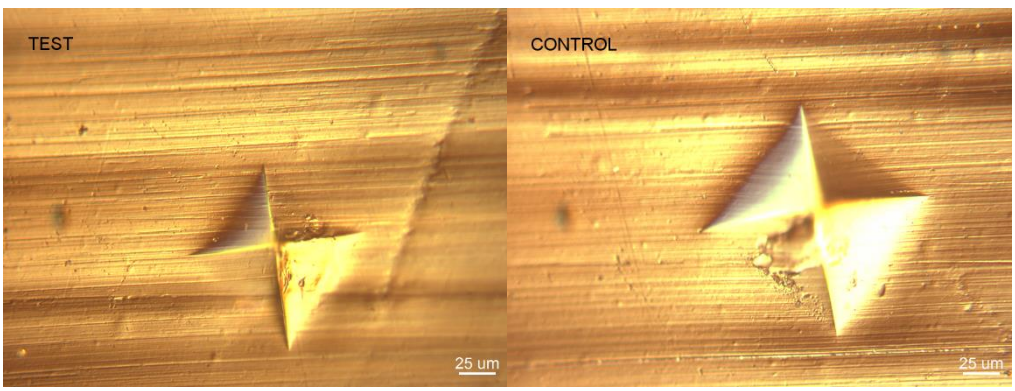

Figure 5: Indentation of test (left) and control (right) sample of V_f=15% under 55g load

Figure 5 shows typical indentations on 15% V_f composite samples. Clearly, the control sample shows a larger indentation than on the test sample, indicating that the test sample has a greater hardness value. This effect has been observed on all samples at both V_f values.

The microhardness test results are presented in Table 1 and Figure 6 and two observations can be made. First, the microhardness of the test samples is increased by 20% and 33% over the control samples at 2.0% and 15% V_f respectively. This effect can be attributed to the residual compressive stresses within the matrix, which are therefore in the surface of the sample, and these must impede indentation forces. Since the load applied during microhardness testing must overcome these lateral stresses, a smaller indentation is produced.

V_f (%)	Microhardness ± SE		Increase (%)
	Test	Control	
0	11.33 ± 0.12		
2.0	9.98 ± 0.05	8.33 ± 0.26	20
15	8.33 ± 0.61	6.24 ± 0.13	33
100*	13.45 ±0.57		

Table 1: Microhardness values of test (prestressed) and control (non-prestressed) samples at different fibre volume fractions; SE = standard error of the mean (10 readings). *Measurements from nylon 6,6 monofilament cross-sections.

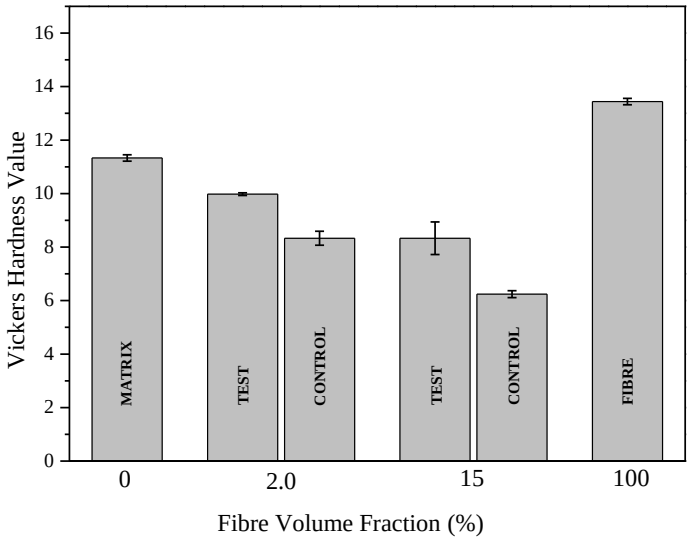

Figure 6: Microhardness of test (prestressed) and control (non-prestressed) samples at different fibre volume fractions. 'Fibre' corresponds to measurements from nylon 6,6 monofilament cross sections. Error bars represent standard error of the mean.

The second observation is that microhardness decreases with increasing fibre volume fraction. This effect can be observed for both prestressed and non-prestressed samples, which is in contrast with the conclusion of that the hardness of a composite is considerably higher than that of a neat matrix due to the introduction of stiff fibres [21, 22]. Although speculative, possible explanations for the observed microhardness reduction in our work include (i) additional porosity from air trapped between fibres during the moulding process and (ii) the presence of fibre-matrix interfaces, which in this case may affect the mechanical properties of the adjacent matrix regions; i.e. interphase effects.

As described in Section 3.3, the changes in indentation over time were observed and

measured with a Nikon optical microscope in DIC mode, which could produce three-dimensional pictures of indentations. This facilitated identification and measurement and Figures 7 and 8 show (in 2-D) examples of these images. At 7 minutes after load removal, both figures (i.e. test and control samples) show the edges of the pyramidal indentations are straight. As time progresses however, the test sample (Figure 7) starts to show some shrinkage of the indentation surfaces towards the centre, so that the edges become inwardly concaved, resulting in a more star-shaped indentation; the indentation diagonals are not significantly affected. Since the indentation in the control sample (Figure 8) remains closer to a regular pyramid with time, the indentation changes observed in the test sample must be attributed to prestress effects.

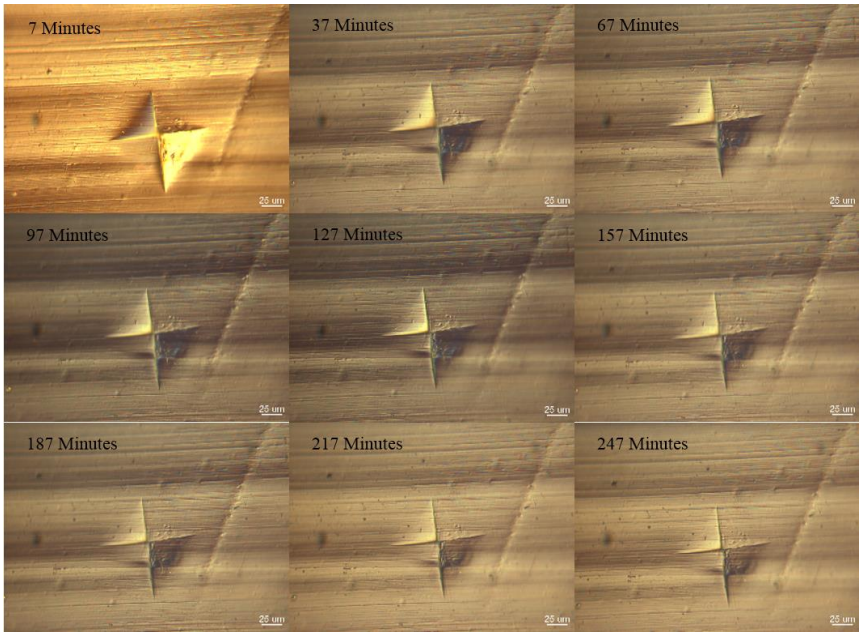

Figure 7: Indentation changes with time on a test (prestressed) sample, 15% V_f.

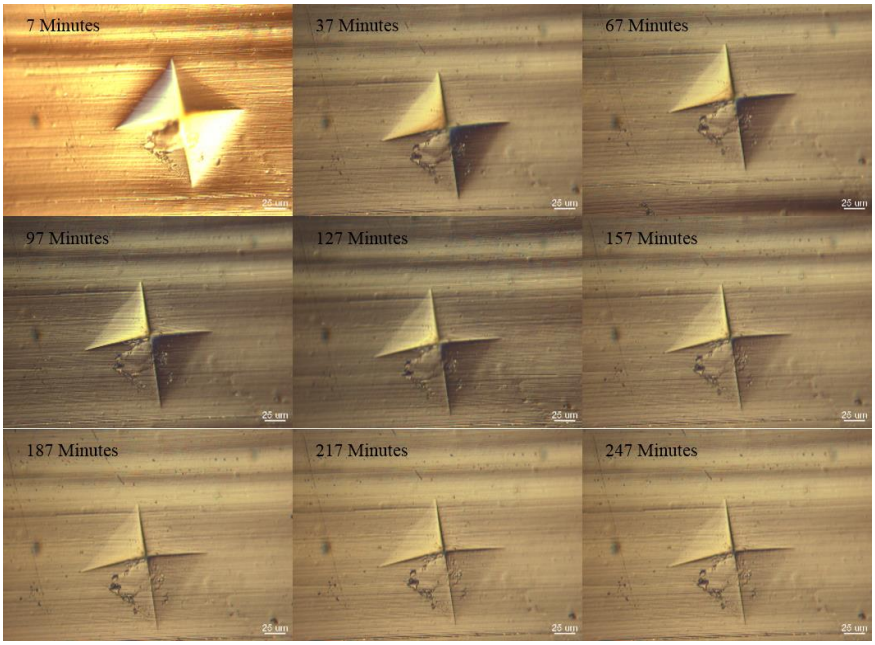

Figure 8: Indentation changes with time on a control (non-stressed) sample, 15% V_f.

5 Conclusions

By performing SEMME (scanning electron microscope mirror effect) and Vickers microhardness tests on viscoelastically prestressed samples and their control (non-prestressed) counterparts, we have found that the prestressed samples demonstrate a greater aptitude for diffusing trapped charges and also give higher hardness values. Specifically:

1. For samples with 2% fibre volume fraction, SEMME analysis showed that the prestressed samples produced a steeper gradient than that of the control samples in the linear region of the mirror plots, indicating that the prestressed samples trapped 26% fewer charges than the control samples, which implies that the prestressed samples possess higher interfacial strength. This may be due to the prestress effect reducing the availability of interfacial defects that are capable of trapping charges and the reduction in defects improves fibre-matrix interfacial adhesion.
2. The results from Vickers microhardness showed that the prestressed samples exhibited higher hardness values than their control counterparts. The prestressed sample microhardness values increased by 20% and 33% over control samples at 2.0% and 15% fibre volume fractions respectively. This effect can be attributed to compressive stresses within the matrix, which must impede indentation forces. With an increase in fibre volume fraction however, the microhardness of both prestressed and control samples decreases. This may be caused by additional porosity from air trapped within fibres and the fibre-matrix interface regions having a localised effect on matrix mechanical properties. Also, due to the prestress within VPPMCs, indentation geometry becomes progressively more star-shaped while that of the control samples remains closer to a regular pyramidal shape.

Acknowledgements

Two of the authors (C.G., B.W.) would like to thank the China Scholarship Council for financial support. School of Engineering support (PhD degree fee waiver for B.W.) is gratefully acknowledged. Special thanks also to Garry Robinson for technical support.

REFERENCES

[1] K.S. Fancey, Prestressed polymeric composites produced by viscoelastically strained nylon 6,6 fibre reinforcement. *Reinforced Plastics and Composites*, **19**, 1251-1266, 2000.

[2] K.S. Fancey, Fibre-reinforced polymeric composites with viscoelastically induced prestress. *Advanced Materials*, **37**, 21-29, 2005.

[3] J.W.C. Pang, K.S. Fancey, An investigation into the long-term viscoelastic recovery of Nylon 6,6 fibres through accelerated ageing. *Materials Science and Engineering A*, **431**, 100-105, 2006.

[4] K.S. Fancey, Viscoelastically prestressed polymeric matrix composites –potential for useful life and impact protection. *Composites Part B*, **41**, 454-461, 2010.

[5] A. Fazal, K.S. Fancey, Viscoelastically prestressed polymeric matrix composites –effects of test span and fibre volume fraction on Charpy impact characteristics. *Composites Part B*, **44**, 472-479, 2013.

[6] J.W.C. Pang, K.S. Fancey, The flexural stiffness characteristics of viscoelastically prestressed polymeric matrix composites. *Composites Part A*, **40**, 784-790, 2009.

[7] J.W.C. Pang, K.S. Fancey, Analysis of the tensile behaviour of viscoelastically prestressed polymeric matrix composites. *Composites Science and Technology*, **68**,

1903-1910, 2008.
[8] A.S. Hadi, J.N. Ashton, On the influence of pre-stress on the mechanical properties of a unidirectional GRE composite. *Composite structures*, **40**, 305-311, 1997.
[9] S. Motahhari, J. Cameron, Impact strength of fibre pre-stressed composites. *Reinforced Plastics and Composites*, **17**, 123-130, 1998.
[10] S. Motahhari, J. Cameron, Fibre prestressed composites: improvement of flexural properties through fibre prestressing. *Reinforced Plastics and Composites*, **18**, 279-288, 1999.
[11] K.S. Fancey, A. Fazal, Prestressed polymeric matrix composites: Longevity aspects. *Polymer Composites*, DOI: 10.1002/pc.23387, in press, 2015.
[12] H. Cui, M. Guan, Y. Zhu, Z. Zhang, The flexural characteristics of prestressed bamboo slivers reinforced parallel strand lumber (PSL). *Key Engineering Materials*, **517**, 96-100, 2012.
[13] A. Fazal, K.S. Fancey, Viscoelastically generated prestress from ultra-high molecular weight polyethylene fibres. *Materials Science*, **48**, 5559-5570, 2013.
[14] A. Fazal, K.S. Fancey, UHMWPE fibre-based composites: Prestress-induced enhancement of impact properties. *Composites: Part B*, **66**, 1-6, 2014.
[15] J.W.C. Pang, B.M. Lamin, K.S. Fancey, Force measurement from viscoelastically recovering Nylon 6,6 fibres. *Materials Letters*, **62**, 1693-1696, 2008.
[16] B. Kchaou, C. Turkic, M. Salviab, Z. Fakhfakha, D. Treheux, Role of fibre-matrix interface and fibre direction on dielectric behaviour of epoxy composites. *Composites Science and Technology*, **64**, 1467-1475, 2004.
[17] B. Kchaou, M. Salvia, B. Beaugiraud, D. Juvé, Z. Fakhfakh, D. Treheux, Mechanical and dielectric characterization of hemp fibre reinforced polypropylene (HFRPP) by dry impregnation. *Express Polymer Letters*, **4**, 171-182, 2010.
[18] B. Vallayer, G. Blaise, D. Treheux, Space charge measurement in a dielectric material after irradiation with a 30kV electron beam: Application to single-crystal oxide trapping properties. *Review of Scientific Instruments*, **70**, 3102-3112, 1999.
[19] I.M. Low, G. Paglia, C. Shi, Indentation response of viscoelastic materials. *Journal of Applied Polymer Science*, **70**, 2349-2352, 1998.
[20] I.M. Low, Effects of load and time on the hardness of a viscoelastic polymer. *Materials Research Bulletin*, **33**, 1753-1758, 1998.
[21] T. Ramanathan, E. Schulz, K. Subramanian, Determination of micro-hardness and elastic modulus in the transcrystalline zone of carbon fibre/PPS composite using a knife edge indentor. *Composites Science and Technology*, **65**, 1-7, 2005.
[22] W.P. Paplham, J.C. Seferis, F.J. Baltá-Calleja, H.G. Zachmann, Microhardness of carbon fibre reinforced epoxy and thermoplastic polyimide composites. *Polymer Composites*, **16**, 424-428, 1995.